Indian Journal of Science and Technology, *Vol 10(17), DOI: 10.17485/ijst/2017/v10i17/104954, May 2017*
ISSN (Print) : 0974-6846
ISSN (Online) : 0974-5645

Assessment of Post Annealing on Magnetic Properties of Co Doped In_2O_3 in Hydrogen Atmosphere using Cluster Analysis

Rana Mukherji[1]*, Vishal Mathur[1], Arvind Samariya[2] and Manishita Mukherji[3]

[1]The ICFAI University, Jaipur – 302031, Rajasthan, India; rana.mukherji@gmail.com, wishalmathur@gmail.com
[2]S. S. Jain Subodh P.G. College, Jaipur – 302004, Rajasthan, India; phy.arvind@gmail.com
[3]Amity University Rajasthan, Jaipur – 303007, Rajasthan, India; manishita@outlook.com

Abstract

Objective: Multivariate statistical analysis viz. Cluster Analysis (CA) was performed to validate the experimental findings. **Methods/Statistical Analysis**: The $(In_{0.955}CO_{0.045})_2O_3$ samples were concocted by the typical solid state reaction route. The resulting materials were pelletized and sintered in hydrogen atmosphere. Subsequently, hydrogenated pallets were de-hydrogenated by further heating for 7h in air. The samples were thoroughly characterized using X-ray diffraction. FULLPROF Program is used to refine the crystalline structures. Magnetic hysteresis loops were evaluated using Vibrating Sample Magnetometer (VSM) at room temperature. Hierarchical CA was accomplished on the normalized data set (samples) by means of the Ward's method, using Euclidean distances as a measure of similarity. **Findings**: The X-Ray Diffraction (XRD) study confirmed the formation of cubic bixbyite structure for In_2O_3, $(In_{0.955}Co_{0.045})_2O_3$and $(In_{0.955}Co_{0.045})_2O_3$:H samples. The magnetic study at Room Temperature (RT) confirms that pure In_2O_3 is diamagnetic and turns to paramagnetic upon Co doping. Furthermore, it was found that the ferromagnetic property is evidently induced by post-annealing in hydrogen atmosphere. This investigation also depicts that after further long heating, the sample again resumes its paramagnetic behaviour. CA grouped the five samples into three groups based on similarities of magnetic characteristics as diamagnetic, paramagnetic and ferromagnetic. The statistical study validates the experimental findings. **Improvements/Applications:** CA helps in the corroboration of data matrices of experimental findings to better understand the influence of hydrogen annealing on magnetic properties of cobalt doped indium oxide.

Keywords: Cluster Analysis, Hydrogen, In_2O_3, Magnetic Properties, Post-Annealing

1. Introduction

Diluted Magnetic Semiconductors (DMSs) have newly engrossed wide attention for their promising spintronics capability, whereby the charge and spin of electrons are accommodated into a single function, causing in encouraging magnetic, magneto-electric, magneto-optical and other properties, thus, are also referred as semi-magnetic semiconductors[1–4].

Oxide DMS offers widespread band gap, high Curie Temperature (T_c) and carrier concentration. These are also easy to prepare at low material cost. It has been observed that oxygen vacancies are one of the key factors for the induced room temperature ferromagnetism[5–8]. Various experimental and theoretical investigations were proposed on the magnetic properties of Transition Metal (TM)-doped TiO_2[9,10], ZnO[11–18], SnO_2[19–21], In_2O_3[7,8,22,23] etc.

*Author for correspondence

Among these, In_2O_3 is the foremost oxide material taken in to consideration by number of researchers[24–26]. The In_2O_3 exhibits a cubic bixbyite crystal structure. It is a transparent, n-type degenerate semiconducting material with a direct band gap of ~3.75 eV[27]. It is interesting if one could comprehend ferromagnetism in In_2O_3 matrix when compared to other DMSs.

The present work focuses on impact of postsintering on magnetic aspects of Co doped In_2O_3 in hydrogen atmosphere. A multivariate technique viz. Cluster Analysis (CA) is utilised for elucidation of the data matrices of all In_2O_3 samples which proves the sustenance of the findings.

2. Materials and Methods

2.1 Experimental Details

Typical Solid state reaction route is utilised to concocte the composition of $(In_{0.955}Co_{0.045})_2O_3$ using In_2O_3 (99.99% pure: Aldrich) and Co_2O_3 (99.999% pure: Alfa Aesar) powders[28]. Now the samples are taken in a quartz tube and placed in reduction furnace for post-annealing in presence of hydrogen for ~5 hours[1] at around 550°C Samples were structurally analysed through X-Ray Diffraction (XRD) technique at ambient temperature of 300 K through PHILIPS X'PERT XRD equipped with CuKα radiation. The scans have been captured from scattering angle 20° to 90° with a step size of 0.02°. The Rietveld profile refinements program, FULLPROF, is used to refine the crystalline structures[29]. Field dependent magnetization analyses have been taken at 300 K using Vibrating Sample Magnetometer (VSM).

2.2 Cluster Analysis

Cluster analysis is an investigative data analysis tool for elucidating categorization enigmas. Its aim is to classify instances, cases, data, objects, variables etc. into groups or clusters. The subsequent clusters of variables should show high internal homogeneity and external heterogeneity[30]. Hierarchical Cluster analysis, the utmost prevailing method, begins with every instance or case in a distinct cluster and unites clusters together gradually up till only a single cluster remnants[31]. The euclidean distance typically delivers the similarity among two samples. The distance can be computed by the difference amongst analytical values obtained from the samples. The euclidean distance between two objects (monitoring point samples), i and j, is specified as:

$$d_{i,j}^2 = \sum_{k=1}^{m} (z_{i,k} - z_{j,k}) \quad (1)$$

Where $d_{i,j}$ represents the Euclidean distance, $z_{i,k}$ and $z_{j,k}$ are the values of variable k for object i and j, respectively, and m is the number of variables.

The outcomes of the clustering method are best defined by a binary tree or Dendogram. The Dendogram delivers a pictographic précis of clustering methods, presenting a graphic representation of the groups and their proximity, with an affected decrease in dimensionality of the actual data. The data standardisation should be an important step to follow in cluster analysis (mean = 0; variance = 1)[32,33]. It will also minimalize the influences of scale of measurement of data. STAISTICA 7.0 software had been used to perform all the statistical calculations.

3. Results and Discussion

3.1 Structural Properties

Figure 1a evinces the XRD scans of the undoped In_2O_3, $(In_{0.955}Co_{0.045})_2O_3$ and the hydrogenated $(In_{0.955}Co_{0.045})_2O_3$:H samples. All the Bragg's peaks of the samples are observed well indexed to the single phase cubic bixbyite or C-type rare earth of In_2O_3 crystalline which validates the non-occurrence of subordinate phases and Co cluster formation. FULLPROF Program is used to assess Rietveld profile refinements of XRD patterns of $(In_{0.955}Co_{0.045})_2O_3$ as shown in Figure 1b[28]. The refinement outcomes ratify that Co^{2+} ions replace the In^{3+} site and no structural change has been noted after the annealing in hydrogen atmosphere and then re-heating. A slight cell volume contraction is observed on Co doping (V= 1035.4 Å^3 for pure In_2O_3 and V= 1029.5 Å3 for 4.5% Co doped sample), due to a minor divergence in ionic radii of the Co and In ions (Co^{2+} :0.745Å and In^{3+} :0.80 Å)[26,27]. When the hydrogenated samples are reheated for 7 hours, interestingly, the oxygen contents again acquire their as-prepared values. Quantum Design (Versa Lab, USA) Vibrating Sample Magnetometer (VSM) is used to analyse the Magnetization (M-H) measurements.

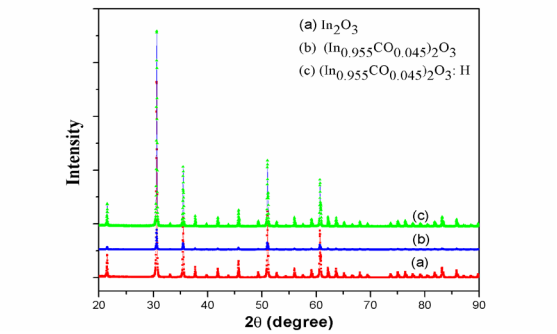

Figuire 1a. XRD scans of In_2O_3,$(In_{0.955}Co_{0.045})_2O_3$ and $(In_{0.97}Co_{0.03})_2O_3$:H samples.

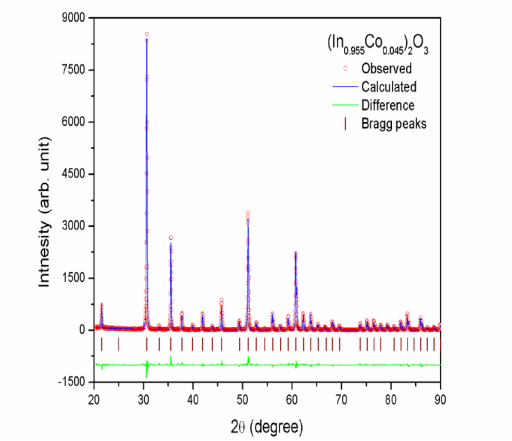

Figure 1b. Refined XRD scans of $(In_{0.955}Co_{0.045})_2O_3$ sample.

3.2 Magnetization Data with Clustering Analysis

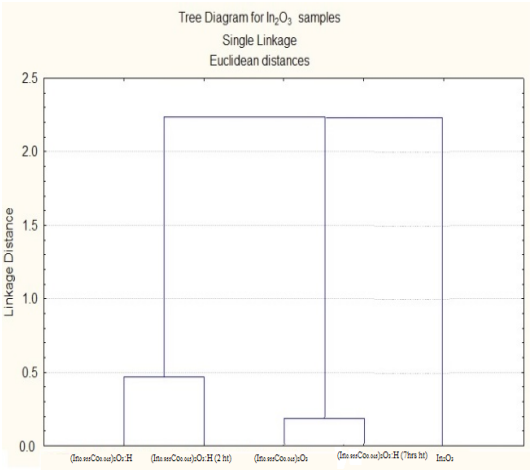

Figure 2. Dendrogram of Cluster Analysis of In_2O_3 samples.

Clustering method performs a critical function in information evaluation. On this paper we have validated the findings of impact of hydrogen sintering on magnetic attributes of Co doped In_2O_3 in the form of clustering[34]. The Figure 2 shows the Dendogram derived by clustering the In_2O_3 data sets (including pure, Co-doped and hydrogenated and then re-heated In_2O_3 samples). The Dendogram encompasses three clusters viz. are group 1 is contained of pure In_2O_3. It is well known that pure undoped In_2O_3 is diamagnetic material. The Figure 3 also reveals the un-doped In_2O_3 sample noted at 300 K as observed in the magnetization versus applied field (M-H) curves (Figure 5) Thus, group 1 validates a strong diamagnetic behaviour of pure In_2O_3. Figure 4(a) shows the magnetization of the $(In_{0.955}Co_{0.045})_2O_3$samples air-sintered at 550 °C as a function of an applied magnetic field H (M–H plots). The samples exhibit paramagnetic behaviour probably due to replacement of In ions by notable amount of Co ions in In_2O_3 after the solid-state reaction reaches completion at 550 °C. Figure 4(b) shows hysteresis loop of $(In_{0.955}Co_{0.045})_2O_3$: H which exhibit obvious ferromagnetic behaviour. The saturation magnetic moment also rises to significant value of 3.33 emu/g (300 K). The coercivity and remanence are also shown note worthy values of 0.0242 T and 0.177 emu/g respectively at 300 K. These outcomes are possibly due to the inclination in number of oxygen vacancies after hydrogenation. Thus, the finding also specifies that the oxygen vacancies portray a pivotal role in developing ferromagnetism in the annealed samples[35]. Hence, the hydrogenated sample comprised in group 3 in Dendogram (Figure 2) which represents the cluster of ferromagnetic behaviour pellets.

Sample $(In_{0.955}Co_{0.045})_2O_3$:H was then annealed till two hours at 550°C in air. The saturation magnetic moment decreases from 3.33 emu/g to 0.111 emu in 300 K. But still the sample acquires the weak ferromagnetic behaviour as shown in Figure 4(c). Thus, the reheated sample also categorised in group 3 in the Dendogram.

The hydrogenated sample further heated for longer duration of almost seven hours. The M-H curve for the heated sample (Figure 4 (d)) shows that the $(In_{0.955}Co_{0.045})_2O_3$:H sample is eventually retained to the paramagnetic state after the long heating. Consequently, it resembles in group 2 of the Dendogram.

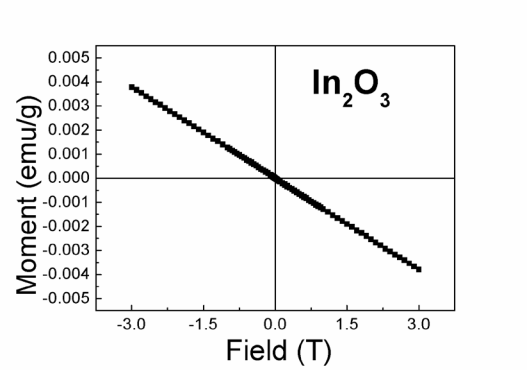

Figure 3. The M-H plot for In_2O_3.

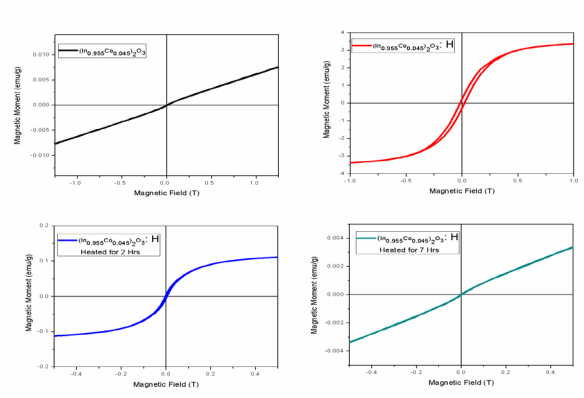

Figure 4. M-H plots registered at 300 K for **(a)** $(In_{0.955}Co_{0.045})_2O_3$ **(b)** $(In_{0.955}Co_{0.045})_2O_3$:H **(c)** Heated sample (2 hours) $(In_{0.955}Co_{0.045})_2O_3$:Hand **(d)** Heated sample (7 hours) $(In_{0.955}Co_{0.045})_2O_3$:H.

4. Conclusion

In this study, cluster analysis (z-transformation of the input data, similarity measure-euclidean distance) is plied to categorize all the In_2O_3 samples. Based on the assessment, the In_2O_3 samples are legiblycleaved into three groups - diamagnetic, paramagnetic and ferromagnetic behaviour of the pure, Co-doped, post annealed under hydrogen atmosphere and then re-heated In_2O_3 samples. Dendogram obtained from cluster analysis technique also authenticates the outcomes of the VSM.

5. References

1. Wolf SA, Awschalom DD, Buhrman RA, Daughton JM, Von Molnar S, Roukes ML, Chtchelkanova AY, Treger DM. Spintronics: A spin-based electronics vision for the future. Science. 2001 Nov 16; 294(5546):1488-95. Crossref PMid:11711666
2. Sarma SD, Fabian J, Hu X, Žutic I. Spin electronics and spin computation. Solid State Communications. 2001 Jul 25; 119(4):207-15. Crossref
3. Yan HL, Zhong XL, Wang JB, Xu JQ, Yu BH. Evolution of local structure and room temperature ferromagnetism in Co-doped ZnO nanorods. Scripta Materialia. 2012 Mar 31; 66(5):304-6. Crossref
4. Iqbal J, Janjua RA, Jan T. Structural, optical and magnetic properties of Co-doped ZnO nanoparticles prepared via a wet chemical route. International Journal of Modern Physics B. 2014 Oct 10; 28(25):1450158. Crossref
5. Xiao ZR, Fan XF, Guan LX, Huan CH, Kuo JL, Wang L. First-principles study of the magnetization of oxygen-depleted In2O3 (001) surfaces. Journal of Physics: Condensed Matter. 2009 Jun 4; 21(27):272202. Crossref PMid:21828483
6. Wu K, Gu S, Tang K, Zhu S, Zhou M, Huang Y, Xu M, Zhang R, Zheng Y. Ferromagnetism induced by oxygen-vacancy complex in (Mn, in) codoped ZnO. Physica B: Condensed Matter. 2012 Jul 1; 407(13):2429-33. Crossref
7. Babu SH, Kaleemulla S, Rao NM, Krishnamoorthi C. Indium oxide: A transparent, conducting ferromagnetic semiconductor for spintronic applications. Journal of Magnetism and Magnetic Materials. 2016 Oct 15; 416:66-74. Crossref
8. Mukherji R, Mathur V, Samariya A, Mukherji M. Review on transition metal doped In2O3 based diluted magnetic semiconductors. The IUP Journal of Electrical and Electronics Engineering. 2016 Oct; 4(1):16-31.
9. NINA B. Room temperature ferromagnetism study of TiO2 based magnetic semiconductors by pulsed laser deposition [Doctoral dissertation].
10. Manivannan A, Glaspell G, Dutta P, Seehra MS. Nature of the reversible paramagnetism to ferromagnetism state in cobalt-doped titanium dioxide. Journal of Applied Physics. 2005 May 15; 97(10):10D325.
11. Dietl T, Ohno H, Matsukura F, Cibert J, Ferrand D. Zener model description of ferromagnetism in zinc-blende magnetic semiconductors. Science. 2000 Feb 11; 287(5455):1019-22. Crossref PMid:10669409
12. Xu XH, et al. Carrier-induced ferromagnetism in n-type ZnMnAlO and ZnCoAlO thin films at room temperature. New Journal of Physics. 2006; 8(8):135. Crossref
13. Gandhi V, Ganesan R, Abdul Rahman Syedahamed HH, Thaiyan M. Effect of cobalt doping on structural, optical and magnetic properties of ZnO nanoparticles synthesized by co-precipitation method. The Journal of Physical Chemistry C. 2014 Apr 24; 118(18):9715-25. Crossref

14. Thakare VP, Game OS, Ogale SB. Ferromagnetism in metal oxide systems: interfaces, dopants and defects. Journal of Materials Chemistry C. 2013; 1(8):1545-57. Crossref
15. Zhang F, Chao D, Cui H, Zhang W, Zhang W. Electronic structure and magnetism of Mn-Doped ZnO nanowires. Nanomaterials. 2015 May 27; 5(2):885-94. Crossref PMid:28347042 PMCid:PMC5312896
16. Straumal BB, Protasova SG, Mazilkin AA, Schutz G, Goering E, Baretzky B, Straumal PB. Ferromagnetism of zinc oxide nanograined films. Jetp Letters. 2013 May 1; 97(6):367-77. Crossref
17. Akilan T, Srinivasan N, Saravanan R, Chowdury P. Structure of vanadium-doped zinc oxide, Zn1–XVxO. Materials and Manufacturing Processes. 2014 Jul 3; 29(7):780-8. Crossref
18. El Ghoul J. Synthesis, structural and optical properties of nanoparticles (Al, V) co-doped zinc oxide. Bulletin of Materials Science. 2016 Feb 1; 39(1):7-12. Crossref
19. Ogale SB, Choudhary RJ, Buban JP, Lofland SE, Shinde SR, Kale SN, Kulkarni VN, Higgins J, Lanci C, Simpson JR, Browning ND. High temperature ferromagnetism with a giant magnetic moment in transparent co-doped SnO2–δ. Physical Review Letters. 2003 Aug 15; 91(7):077205. Crossref PMid:12935053
20. Fitzgerald CB, Venkatesan M, Douvalis AP, Huber S, Coey JM, Bakas T. SnO2 doped with Mn, Fe or Co: room temperature dilute magnetic semiconductors. Journal of Applied Physics. 2004 Jun 1; 95(11):7390-2. Crossref
21. Coey JM, Douvalis AP, Fitzgerald CB, Venkatesan M. Ferromagnetism in Fe-doped SnO2 thin films. Appl Phys Lett. 2004 Jan 16. Crossref
22. Philip J, Punnoose A, Kim BI, Reddy KM, Layne S, Holmes JO, Satpati B, Leclair PR, Santos TS, Moodera JS. Carrier-controlled ferromagnetism in transparent oxide semiconductors. Nature Materials. 2006 Apr 1; 5(4):298-304. Crossref
23. He J, Xu S, Yoo YK, Xue Q, Lee HC, Cheng S, Xiang XD, Dionne GF, Takeuchi I. Room temperature ferromagnetic n-type semiconductor in (In1-xFex)2O3-s. Applied Physics Letters. 2005; 86(5):52503. Crossref
24. Xu XH, Jiang FX, Zhang J, Fan XC, Wu HS, Gehring GA. Magnetic and transport properties of n-type Fe-doped In2O3 ferromagnetic thin films. Applied Physics Letters. 2009; 94:212510. Crossref
25. Singhal RK, Samariya A, Kumar S, Sharma SC, Xing YT, Deshpande UP, Shripathi T, Saitovitch E. A close correlation between induced ferromagnetism and oxygen deficiency in Fe doped In2O3. Applied Surface Science. 2010 Nov 15; 257(3):1053-7. Crossref
26. Pooryusef K, Kangarlou H. Effects of temperature on structural properties of indium oxide thin layers produced by CBD method. Indian Journal of Science and Technology. 2015 Dec 3; 8(35). Crossref
27. Ma RR, Jiang FX, Qin XF, Xu XH. Effects of oxygen vacancy and local spin on the ferromagnetic properties of Ni-doped In2O3 powders. Materials Chemistry and Physics. 2012 Feb 15; 132(2):796-9. Crossref
28. Singhal RK, Samariya A, Xing YT, Kumar S, Dolia SN, Deshpande UP, Shripathi T, Saitovitch EB. Electronic and magnetic properties of Co-doped ZnO diluted magnetic semiconductor. Journal of Alloys and Compounds. 2010 Apr 30; 496(1):324-30. Crossref
29. Rodriguez-Carvajal J. FULLPROF version 3.0. 0. Laboratorie Leon Brillouin, CEA-CNRS. 2003.
30. McGarigal K, Cushman SA, Stafford S. Multivariate statistics for wildlife and ecology research. Springer Science and Business Media. 2013 Dec 1.
31. McKenna JE. An enhanced cluster analysis program with bootstrap significance testing for ecological community analysis. Environmental Modeling and Software. 2003 Apr 30; 18(3):205-20. Crossref
32. JI NK, Das M, Mukherji R, Kumar RN. Assessment of heavy metal pollution in macrophytes, water and sediment of a tropical wetland system using hierarchical cluster analysis technique. J International Environmental Application and Science. 2011; 6(1):149-56.
33. Salah EA, Turki AM, Al-Othman EM. Assessment of water quality of Euphrates River using cluster analysis. Journal of Environmental Protection. 2012 Dec 1; 3(12):1269. Crossref
34. Mukherji R, Mathur V, Samariya A, Mukherji M. Multivariate analysis of influence of hydrogenation and re-heating on intrinsic magnetization of Co doped ZnO. Journal of Ovonic Research. 2016 Nov-Dec; 12(6):301-7.
35. Samariya A, Singhal RK. A study of magnetic and electronic correlations in hydrogen-induced room temperature ferromagnetism in co-doped ZnO. Advances in Applied Research. 2010; 2(1):1-3.